

## Development of aluminum (Al5083)-clad ternary Ag–In–Cd alloy for JSNS decoupled moderator

M. Teshigawara <sup>a,\*</sup>, M. Harada <sup>a</sup>, S. Saito <sup>a</sup>, K. Oikawa <sup>a</sup>, F. Maekawa <sup>a</sup>,  
M. Futakawa <sup>a</sup>, K. Kikuchi <sup>a</sup>, T. Kato <sup>a</sup>, Y. Ikeda <sup>a</sup>, T. Naoe <sup>b</sup>, T. Koyama <sup>b</sup>,  
T. Ooi <sup>b</sup>, S. Zherebtsov <sup>b</sup>, M. Kawai <sup>c</sup>, H. Kurishita <sup>d</sup>, K. Konashi <sup>d</sup>

<sup>a</sup> Japan Atomic Energy Agency, Tokai-mura, Naka-gun, Ibaraki 319-1195, Japan

<sup>b</sup> Ibaraki University, 4-12-1 Nakanarusawa-cho, Hitachi, Ibaraki 316-8511, Japan

<sup>c</sup> High Energy Accelerator Research Organization, 1-1, Oho, Tsukuba-shi, Ibaraki 305-0801, Japan

<sup>d</sup> International Research Center for Nuclear Materials Science, Institute for Materials Research (IMR), Tohoku University, Narita-machi, Oarai-machi, Higashi ibaraki-gun, Ibaraki 311-1313, Japan

### Abstract

To develop Ag (silver)–In (indium)–Cd (cadmium) alloy decoupler, a method is needed to bond the decoupler between Al alloy (Al5083) and the ternary Ag–In–Cd alloy. We found that a better HIP condition was temperature, pressure and holding time at 803 K, 100 MPa and 10 min. for small test pieces ( $\phi 22$  mm in dia.  $\times$  6 mm in height). Hardened layer due to the formation of  $\text{AlAg}_2$  was found in the bonding layer, however, the rupture strength of the bonding layer is more than 30 MPa, the calculated design stress. Bonding tests of a large size piece ( $200 \times 200 \times 30$  mm<sup>3</sup>), which simulated the real scale, were also performed according to the results of small size tests. The result also gave good bonding and enough required-mechanical-strength.

© 2006 Elsevier B.V. All rights reserved.

### 1. Introduction

Spallation neutron source facilities in J-PARC [1] (Japan Proton Accelerator Research Complex) project are under construction. Three kinds (coupled, decoupled and poisoned) of hydrogen moderator were adopted [2,3] to provide a pulsed neutron beam with higher neutronic performance as shown

in Fig. 1. For the decoupled and poisoned moderators, a thermal neutron absorber, i.e., decoupler as shown in Fig. 2, is located around the moderator to prevent slow neutrons from flowing into the moderator and to give a neutron beam with a short decay time. The higher cut-off energy of the decoupler, which is called decoupling energy ( $E_d$ ), results in a shorter decay time with a somewhat sacrificed peak intensity as shown in Fig. 3. It is very important for the high-resolution experiment. Fig. 4 shows the powder diffraction pattern simulated using neutron beam pulses with the  $E_d$  of 0.3 and 1 eV from the neutronic calculation [4]. The weak

\* Corresponding author. Tel.: +81 29 282 6217; fax: +81 29 282 6496.

E-mail address: [teshigawara.makoto@jaea.go.jp](mailto:teshigawara.makoto@jaea.go.jp) (M. Teshigawara).

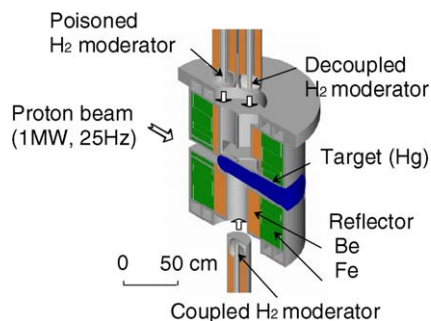


Fig. 1. Cross sectional view of the target-moderator-reflector system for the spallation neutron source in J-PARC.

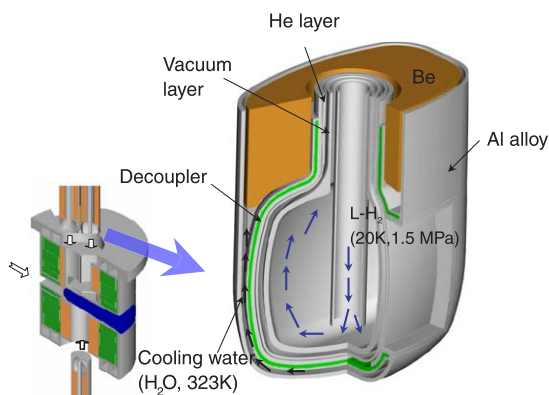


Fig. 2. Structure of the decoupled moderator. The decoupler is installed around the moderator except for the neutron beam extraction window.

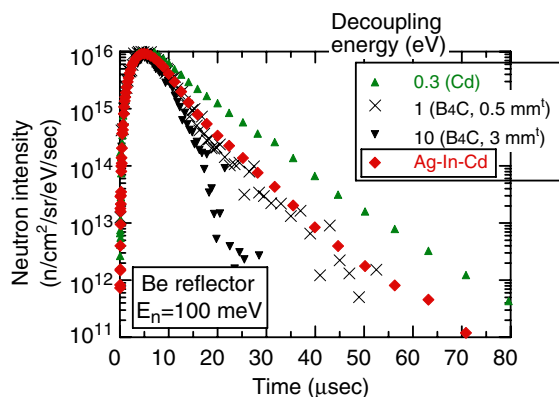


Fig. 3. Neutron beam pulses from the decoupled moderator for various decoupling energies. Higher decoupling energy gives a shorter decay time with somewhat sacrificing the peak intensity.

reflection of near  $d = 0.4693 \text{ \AA}$  shows that it is fully separable as a peak in case of  $E_d$  of 1 eV. The peak separation becomes very important in the analysis of the peak position using Rietveld method to deter-

mine the crystal structure. That is why the pulsed neutron beam with  $E_d$  of more than 1 eV at least is desired by neutron beam users in Japan. The material of the boron (B) system, such as boron carbide ( $B_4C$ ), is already utilized for the decoupler with higher  $E_d$ , however, it is not suitable for a MW class neutron source due to helium (He) void swelling and local heat by  $(n, \alpha)$  reaction. We performed the development of a new material without  $(n, \alpha)$  reaction [5]. It is a combination of materials with different resonance absorption energies. The candidate material is silver–indium–cadmium (Ag–In–Cd), which has an energy-dependence of macroscopic neutron cross-section like  $B_4C$  as shown in Fig. 5. The  $E_d$  of Ag–In–Cd with the thickness of 3 mm reaches at about 1 eV as shown in Fig. 3. The Ag–In–Cd (AIC) alloy sheathed with stainless steel is already utilized for the control rod of pressurized water reactor (PWR). However it is the first trial in a spallation neutron source. The AIC decoupler is installed at around the moderator vessel with the heat deposition of about  $8 \text{ W/cm}^3$  at maximum and near the cooling water flowing as shown in Fig. 2. From a point of view of heat removal and corrosion protection, an AIC plate with the thickness of 3 mm has to be bonded between two plates of the Al alloy, which is the structural material of a moderator or reflector. Especially, from the neutron irradiation point of view, an Al6061-T6 is recommended as a structural material of the moderator [6]. We adopted HIP (Hot Isostatic Pressing) method to obtain the bonding material between the Al6061-T6 and the AIC. We already found the good bonding conditions for the sandwich case [7], which showed that the binary Ag–In and Ag–Cd alloys were clad in Al6061 alloy. The AIC alloy consisted of two binary alloys (Ag–In (15 wt%) and Ag–Cd (35 wt%)) to maximize the Cd composition in the Ag single phase to prevent the Cd depletion by the burn up. HIP treatment affected on the mechanical strength of Al6061-T6 and the T6 heat treatment was needed to recover the mechanical strength of the Al6061 after HIPing. However, exfoliation always occurred in the bonding layer in the sandwich case after T6 heat treatment as shown in Fig. 6. We introduce another Al alloy (Al5083) and ternary Ag–In–Cd alloy. This Al alloy is not a heat-treated material, which does not require the heat treatment to recover the mechanical strength after HIPing, however, it gives a short lifetime for the neutron irradiation as compared with the Al6061-T6 [6]. On the other hand, we found the

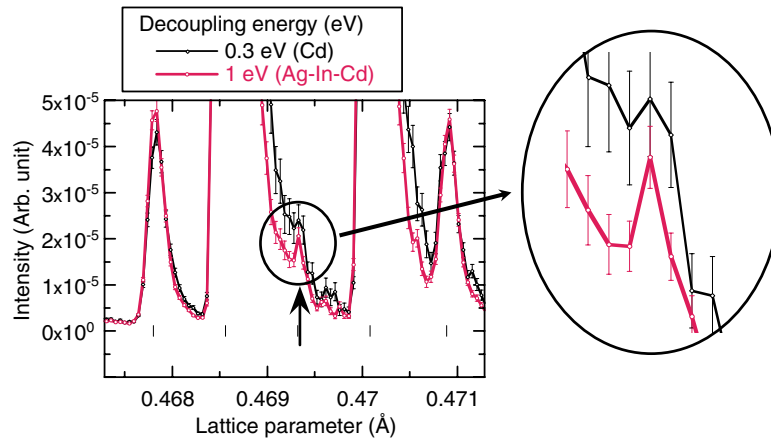


Fig. 4. Powder diffraction pattern simulated using neutron beam pulses with the  $E_d$  of 0.3 and 1 eV from the neutronic calculation. The weak reflection of near  $d = 0.4693 \text{ \AA}$  shows that it is fully separable as a peak in case of  $E_d$  of 1 eV.

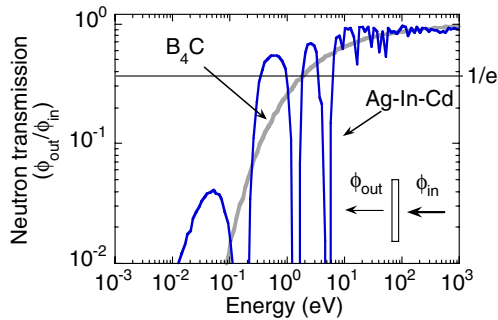


Fig. 5. Neutron transmission profile of Ag–In–Cd with thickness of 3 mm compared with that of  $B_4C$ . Ag–In–Cd alloy is a combination of materials with different resonance absorption energies, which has an energy-dependence of macroscopic neutron cross-section like  $B_4C$ .

necessary Cd composition in the Ag single phase of the ternary AIC to satisfy the required lifetime of the moderator by the neutronic calculation. These bring about no heat treatment after HIPing and the reduction of bonding layer, which resulting in the easier bonding between the Al alloy and the AIC alloy. Especially, the reduction of the bonding layer gives easier fabrication. This report focuses on the establishment of the bonding material between the Al alloy (Al5083) and the ternary AIC.

## 2. Experiment

The HIPing test procedure is briefly shown in Fig. 7.

### 2.1. Sample preparation

The Ag–In (2.5 wt%)–Cd (29.5 wt%) alloy was used for the bonding tests by HIPing. To make ternary Ag–In–Cd (AIC) plates, Ag and necessary amount of In and Cd were melted at about 1373 K in an electric furnace and made into a rod with a diameter of 20 mm in the air. The AIC rod was cut to the plates with a thickness of 3 mm. AIC samples were stored in Al5083 housing capsules (shape: cylindrical, size: approximately 22 mm in outer dia.  $\times$  30 mm in height) contained in a mild steel with thickness of about 0.5 mm. Before storing, samples and Al capsules were polished by an emery paper with up to 1200 grit and cleaned in acetone in an ultra-sonic bath. Each sample contained in the mild steel was heated up to 473 K to

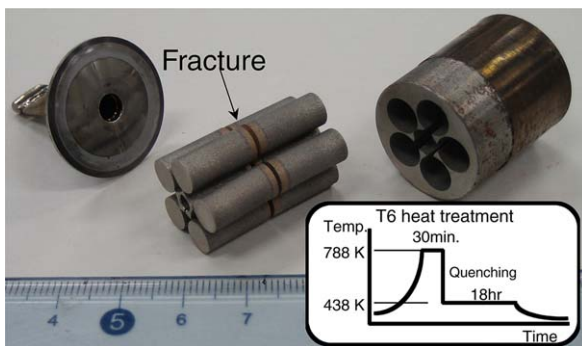


Fig. 6. Fracture always occurred in the bonding layer after T6 heat treatment. Three plates (Ag–In/Ag–Cd/Ag–In alloy) are covered by the Al6061 alloy in the bonding layer, which is called sandwich case. The specimen is pulled out after cutting using a wire electrical discharge machine in the figure.

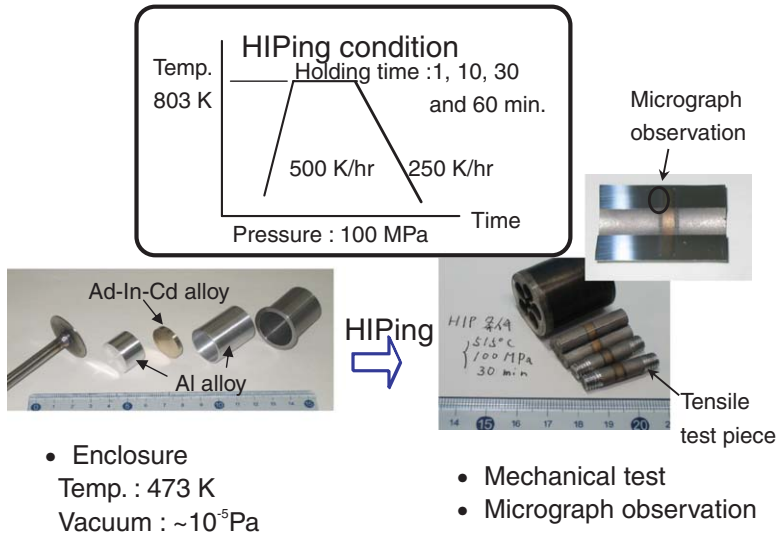


Fig. 7. HIPing test procedure to establish the bonding condition between Al alloy (Al5083) and Ag–In–Cd alloy.

clean the inside surface under  $10^{-5}$  Pa. The outgas was monitored using a quadrupole mass system.

### 2.2. HIPing machine and condition

The HIPing condition, which is mainly based on the previous study [7], is shown in Fig. 7. We used a HIPing machine with a maximum pressure of 200 MPa and a highest temperature of 2273 K. The AIC sample stored in Al alloy capsules was inserted into the alumina crucible and pressurized up to 50 MPa by argon (Ar) gas with 99.9 % purity at room temperature. It was heated up to about 773 K at a rate of 500 K/h. The pressure was increased 100 MPa at about 773 K. After holding for a certain time, the temperature was reduced to room temperature at a rate of 250 K/h.

### 2.3. Microstructure observation and mechanical tests

After HIP treatment, we cut in the crosswise section with respect to bonding layers and polished the sample to observe the microstructures of the interfaces between the Al alloy and AIC, and to measure mechanical properties. Vicker’s micro-hardness tests were conducted in the air with a load of 4.9 N at the outside interface region and 0.49 N at the interface region, respectively, both with a holding time of 15 s. Tensile tests were also performed. The test samples including bonding layer were cut

into a cylindrical shape with 6 mm in diameter using a wire electrical discharge machine.

## 3. Experimental results

### 3.1. HIP treatment of the Ag–In–Cd alloy and the Al5083 alloy

Bonding tests were performed at 803 K and 100 MPa with various holding time (1, 10, 30 and 60 min.). All samples were successfully bonded. Fig. 8 shows a typical micrograph of the bonding

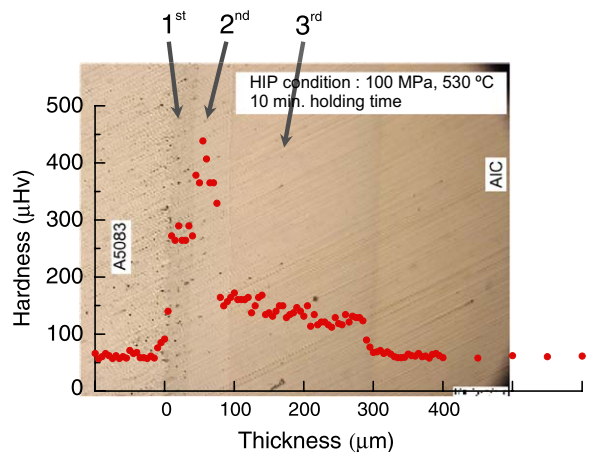


Fig. 8. Typical micrograph and Vicker’s micro hardness result of bonding between Al (Al5083) and Ag–In–Cd alloys after HIPing. Three regions can be seen in the interface region.

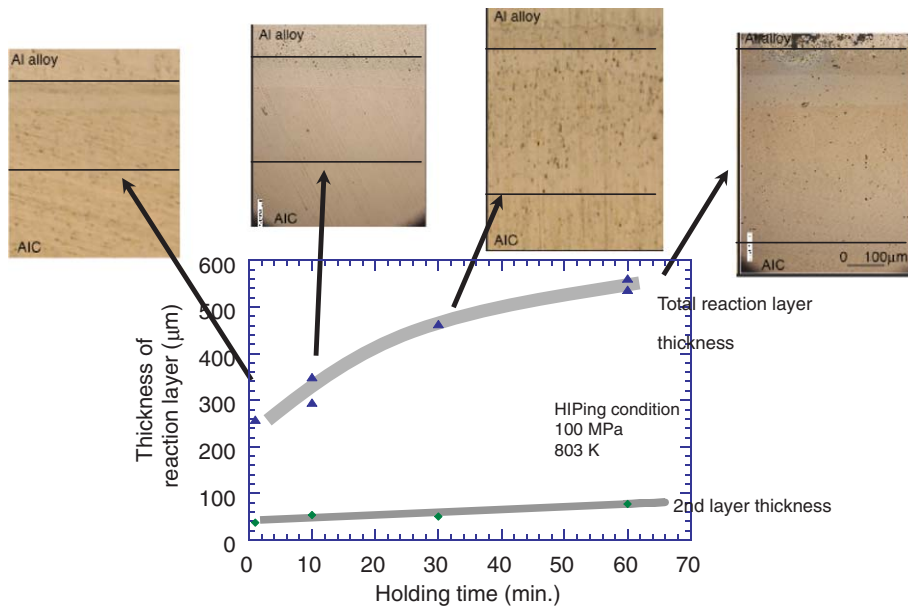


Fig. 9. Holding time dependence of total reaction layer thickness. The thickness of reaction layer increases with holding time. For the reference, micrographs of bonding region are shown above the figure.

region between Al and Ag–In–Cd alloys taken from the case of 10 min. holding time. The reaction layer between Al and Ag–In–Cd alloys consisted of three layers as shown in Fig. 8. The thickness of the reaction layer was about 350  $\mu\text{m}$ . Fig. 9 shows the holding time dependence of total reaction layer thickness. The thickness of the reaction layer increases with holding time as shown in this figure. The total reaction layer thickness is similar to that of previous results (between Al and Ag–In alloy) [7] in the holding time dependence.

### 3.2. Vicker's micro-hardness tests

We performed Vicker's micro-hardness tests. A typical Vicker's micro-hardness test result is shown in Fig. 8. The hardness changed according to reaction layers. The second reaction layer from the Al alloy was most hardened as shown in the figure. The hardest layer could be recognized in the second reaction layer for each HIPed sample. The hardness of each HIPed sample in the second reaction layer was comparable regardless of the different holding time.

### 3.3. Tensile tests

Tensile-test results are shown in Fig. 10. These data almost satisfied the required mechanical strength for any holding times. The required design stress for the decoupler region was evaluated with

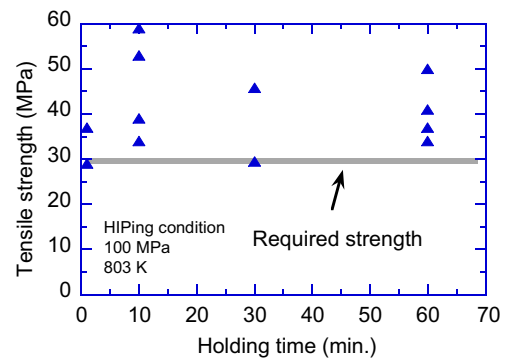


Fig. 10. Holding time dependence of tensile-test results after HIPing.

the ABAQUS code, a finite element method (FEM) calculation code. It can be seen that relatively high mechanical strength was obtained for 10 min. holding time. The typical fractured position is shown in Fig. 11. The fracture occurred at the second reaction layer, which gave most hardened. The samples always fractured at the second reaction layer from Al alloy.

## 4. Discussions

### 4.1. Fracture position in the tensile samples

In the tensile tests, fracture only occurred at the second reaction layer from the Al alloy. The

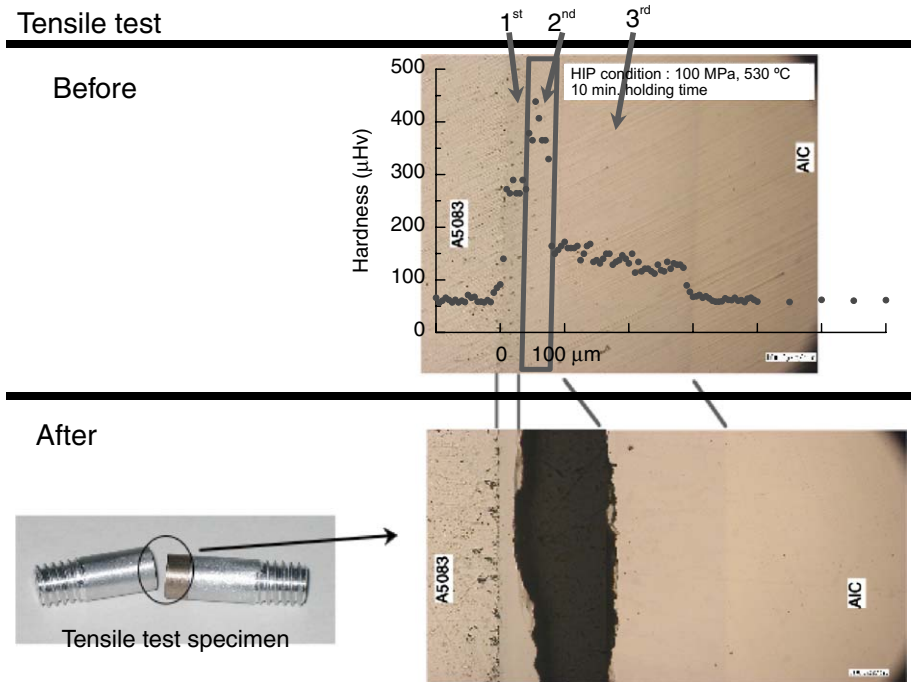


Fig. 11. Fractured position in the tensile sample. Fracture always occurred at second reaction layer from the Al alloy, which showed most hardened.

Vicker’s micro-hardness was highest in the second reaction layer. The hardened layer may be responsible for embrittlement. We performed EDX (energy dispersive X-ray) analysis and X-ray measurement to describe the reason why the fracture occurred at the second layer. Fig. 12 shows the EDX analysis results of the cross section including reaction layer. It can be seen that the composition of Cd and Al were changed according to the phase. The element of In is not shown in the figure though In content 2.5 wt% in the AIC alloy, because the characteristic X-ray from In is almost the same as Cd. It is difficult to distinguish the characteristic X-ray of In from Cd for this analysis. However, the ambiguity from In is less than about 8 at.% in Cd composition. The X-ray measurement result is also shown in Fig. 12. The second reaction layer was revealed by gradual polishing of layers so as to irradiate X-ray to the second reaction layer. Measured peaks corresponded to one of  $\text{Ag}_2\text{Al}$  and  $\text{AgCd}$  with different crystal structure of Ag and Al. The composition change in the diffusion process of HIPing enabled the compound creation of  $\text{Ag}_2\text{Al}$  and  $\text{AgCd}$  in the second layer. The compound creation with different crystal structure in the second layer induced the distortion in the second layer, resulting in hardening

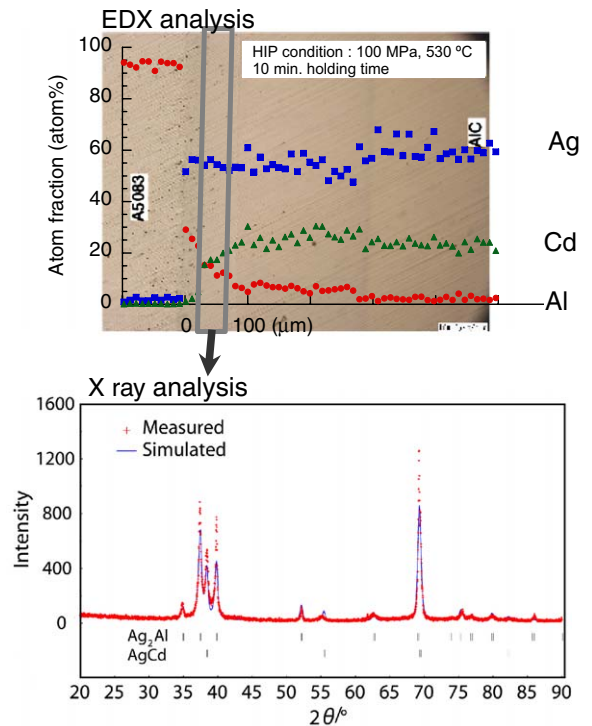


Fig. 12. EDX analysis in the bonding region and X-ray analysis at the second layer from Al alloy.

and embrittlement. That is reason for the fracture always occurred at the second layer in the tensile tests. How is the relationship between the thickness of the second layer and tensile strength? The relationship of the thickness of the second layer and tensile strength is shown in Fig. 13. Roughly speaking, the highest tensile strength can be seen around ~50 μm of the second layer thickness. This shows that the thickness of the second layer should be controlled to ~50 μm to obtain the higher tensile strength. However, the thickness of second layer was not so closely related with total thickness of reaction layer (or holding time) as shown in Fig. 9.

From the neutron irradiation point of view, a thinner reaction layer with required mechanical strength might be desired. Irradiation effects of matrix of Al and AIC have already been revealed [8–10], however, there is no data on the irradiation effects of interfaces between bonding layers, especially between the Al and AIC alloys. Such engineering issues remain to be studied. R&D efforts should be under progress.

4.2. Large size HIPing test

In order to realize the fabrication of the actual decoupler structure, a large sized HIPing test (~200 × 200 × 30 mm<sup>3</sup>) was conducted based on small size results. Because different thermal expansion of Al and AIC alloys may affect the bonding layer in the large size HIPing, resulting in the exfoliation in the bonding layer. The HIPing condition was 100 MPa, 803 K and 10 min. holding time. After HIPing test, ultrasonic wave transmission (UT) and tensile tests were performed to evaluate the bonding condition and mechanical strength. As shown in Fig. 14, the exfoliation was not seen

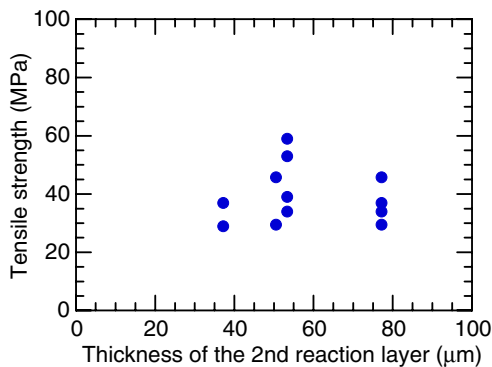


Fig. 13. Dependence of tensile strength on thickness of second reaction layer.

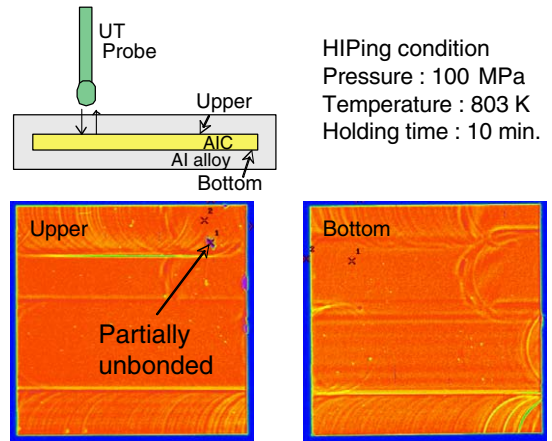


Fig. 14. Ultrasonic wave transmission (UT) tests results after HIPing. The exfoliation was not seen except for a partial unbonded spot. Some scratches can be seen in the UT test result, however, this is due to the scratches by the machining process to remove the mild steel capsule.

except for a partial unbonded spot indicated by the arrow in the figure. Some scratches can be seen in the UT test result, however, this is due to the scratches by the machining process to remove the mild steel capsule, which is the container of Al and AIC alloys.

Fig. 15 shows tensile-test results. The tensile-test specimens were cut into the same shape with a

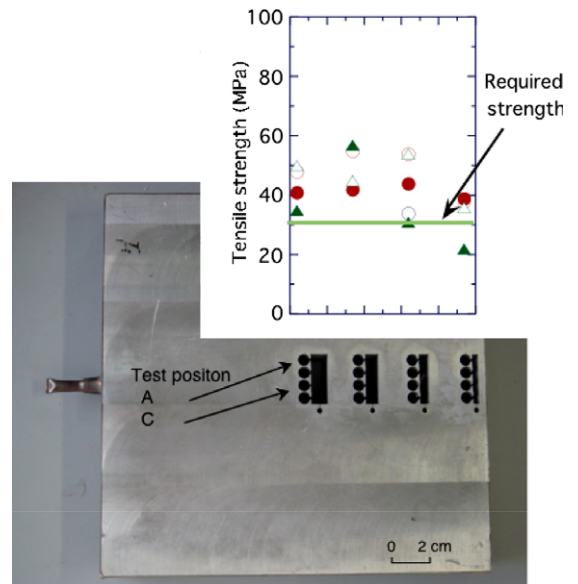


Fig. 15. Tensile-test results after HIPing. The tensile-test specimens were in the same shape of the small ones. The cut location after HIPing is shown in the figure. Obtained tensile strength almost satisfied the required mechanical strength.

smaller size using wire-electrical-discharge-machine. The cut location after HIPing is also shown in Fig. 15.

## 5. Conclusions

We performed bonding tests by HIP (Hot Iso-static Pressing) to establish the bonding condition. We attempted to obtain good bonding conditions between Al5083 and ternary Ag–In–Cd alloys. Since the Al5083 alloy does not need heat treatment to improve the mechanical strength after HIPing but a shorter lifetime compared with the Al6061-T6. Compared with the combination of binary Ag–In and Ag–Cd alloy, which gave good bonding, the ternary alloy reduces bonding layers, resulting in easier bonding and fabrication of decoupler. A good HIP condition was found for small test piece ( $\phi$  20 mm). Though a hardened layer due to the formation of  $\text{AlAg}_2$  is found in the bonding layer, the rupture strength of the bonding layer is more than 30 MPa, which is the calculated design stress. Bonding tests of a large size piece ( $200 \times 200 \times 30 \text{ mm}^3$ ), which simulated the real scale, were also performed according to the results of small size tests. The result also gave good bonding and enough required-mechanical-strength.

## Acknowledgements

The authors would like to thank to the members of the department of Engineering services of Japan

Atomic Energy Research Institute for manufacturing services concerning HIP treatment.

## References

- [1] S. Nagamiya, JAERI-KEK Joint Project on High Intensity Proton Accelerators, Proc. of Int. Conf. Radiation Shielding (ICRS9), J. Nucl. Sci. Technol. (Suppl. 1) (2000) 40.
- [2] M. Teshigawara, M. Harada, T. Kai, T. Teraoku, H. Kogawa, F. Maekawa, N. Watanabe, Y. Ikeda, Development status of moderator–reflector-system in JSNS, in: Proceedings of ICANS-XVI, Dusseldorf-Neuss, Germany, May 12–15, 2003, p. 601.
- [3] High intensity Proton Accelerator Project (J-PARC) Technical Design Report Material and Life Science Experimental Facility, JAERI-Tech 2004-001, (in Japanese).
- [4] M. Harada, M. Teshigawara, N. Watanabe, T. Kai, Y. Ikeda, Optimization of poisoned and unpoisoned decoupled moderators in JSNS, in: Proceedings of ICANS XVI, May 12–15, 2003, Zeughaus, Germany, p. 697.
- [5] M. Harada, S. Saito, M. Teshigawara, M. Kawai, K. Kikuchi, N. Watanabe, Y. Ikeda, Silver–Indium–Cadmium decoupler and liner, in: Proceedings of ICANS-XVI, Dusseldorf-Neuss, Germany, May 12–15, 2003, p. 677.
- [6] K. Farrell, Materials selection for the HFIR cold neutron source, ORNL/TM-99-208.
- [7] M. Teshigawara et al., J. Nucl. Mater. 343 (2005) 154.
- [8] I. Cohen, Development and Properties of silver-base alloys as control rod materials for pressurized water reactors, WAPD-214, AEC Research and Development Report, December 1959.
- [9] A. Strasser, W. Yano, Control rod materials and burnable poisons, An Evaluation of the State of the Art and Needs for Technology Development, July 1980, EPRI NP-1974.
- [10] EPRI-NP-4512 Research Project 1628-4 Final Report March 1986, ‘Lifetime of PWR Silver–Indium–Cadmium Control Rods’.